Ultracold Neutral Plasma Physics at Room Temperature

Joshua Mitchell Wilson

A senior thesis submitted to the faculty of
Brigham Young University
in partial fulfillment of the requirements for the degree of

Bachelor of Science

Scott D. Bergeson, Advisor

Department of Physics and Astronomy

Brigham Young University

August 2013

ABSTRACT

Ultracold Neutral Plasma Physics at Room Temperature

Joshua Mitchell Wilson
Department of Physics and Astronomy
Bachelor of Science

It has been shown that under certain conditions, the characteristics of ultracold neutral plasmas, can be reproduced in laser-produced plasmas at room temperature. We are attempting to see more fully how true this is, by trying to control the electron temperature in a laser-produced plasma. We expected that by decreasing the intensity of our laser when we ionize our gas we would see the expansion of our plasma slow down, and hence deduce that the electron temperature had been lowered. We had difficulty observing this result experimentally. We modeled the system and found that if we increase our laser intensity, we should be able to observe the phenomenon we had hypothesized. The experimental and modeling processes are here outlined, as well as thoughts on how to improve the experiment in the future.

Keywords: ultracold neutral plasmas, interferometry, femtosecond optics, strong-field ionization

ACKNOWLEDGMENTS

Thank you to Dr. Bergeson for his ideas and direction. Thanks to Dr. Justin Peatross for the use of his equipment and for his assistance. Also, thanks to Stephen Rupper for his partnership on this experiment.

This research is funded in part by the National Science Foundation, grant number PHY-0969856

Contents

Table of Contents **iv**

List of Figures **v**

1 Introduction **1**
1.1 Overview 1
1.2 Electron Temperature 2

2 Experiment **4**
2.1 Optical Layout 4
2.2 Alignment Procedures 5
2.3 Data Processing 6
2.4 Preliminary Results 9

3 Modeling **11**
3.1 Theory 11
3.2 Execution 13

4 Conclusions and Outlook **19**

Bibliography **21**

List of Figures

2.1 Optical Set Up for Experiment. 5
2.2 Matlab Graph and Fringes 7
2.3 Sample of Helium Data 10

3.1 Density of Neon Modeled With Known Intensity 14
3.2 Density of Helium Modeled With Known Intensity 15
3.3 Density of Neon Modeled With Higher Intensity 16
3.4 Density of Neon Modeled With Higher Intensity 17

Chapter 1

Introduction

1.1 Overview

A plasma is a collection of charged particles. Since the advent of lasers, a common way to make the ions for a plasma is with a laser. This is done in multiple ways, but the two we are interested in are "photo-electric" ionization and "strong-field" ionization.

In photo-electric ionization, the energy in the electric field of a specific laser wavelength matches the energy that is binding an electron to its parent atom. This causes the electron and the atom to dissociate [1]. It is this sort of ionization that is used in the creation of ultracold neutral plasmas, (UNPs). An UNP is a plasma in which the atoms have been cooled to a very low temperature, as low as $10\,\mu$K, and then ionized [2]. There is currently a lot of exciting research being done in UNPs.

For strong-field ionization the laser is made to be so intense that the electric field of the laser overwhelms the electric field holding the electron to the atom, and the electron just wanders away from its parent [3]. Plasmas made in this fashion are called laser-produced plasmas, (LPPs). It has been shown that under certain conditions the plasmas that are created by strong-field ionization

can behave like UNPs in ways that would allow us to test some of the same dynamics in both plasmas [4].

To test the extent to which this is true, we would like to show that we can control the electron temperature in our LPP by decreasing the intensity of the laser when ionization occurs. If we can do this, we could begin experiments using a series of tailored laser pulses from our laser to try and achieve a high Coulomb coupling parameter

$$\Gamma = \frac{Z^2 q_e^2}{4\pi\varepsilon_0 a_{ws} k_b}$$

where Z is the ionization state, q_e is the electron charge and a_w is the Wigner-Seitz radius [4]. This parameter Γ, is currently of fundamental interest to many physicists, and using a series of pulses from our high-intensity laser source would be a new and possibly more simple way to reach a higher value of Γ then has been possible in UNPs [5].

1.2 Electron Temperature

To know if we are controlling the electron temperature in our plasma, we need to be able to measure the electron temperature. In UNPs, or any photo-electric produced plasma, this is very simple [6]. The electron is bounded by a certain potential energy, and if a gas is ionized using a specific laser energy the electrons in the plasma will have an average kinetic energy given by the difference between the laser energy and the ionization potential. If this energy difference ΔE is known, then the electron temperature can be extracted using $3/2 k_b T_e = \Delta E$.

LPPs are fundamentally different in the way that the plasma is created, and the electron temperature cannot be extracted so easily [7]. It is possible to extract by measuring the rate at which the plasma is expanding once it is created since $v_{exp} m_i = k_b T_e$ [4]. This method is known to be correct under many conditions four UNPs and for LPPs. We wanted to explore the limits of this technique for LPPs and have built our experiment in such a way that do so. This set up, and the

some of the motivation for it, will be discussed in more detail in Chapter 2.

Chapter 2

Experiment

2.1 Optical Layout

In our experiment we use a 35 fs laser with a center wavelength at 800 nm. Figure 2.1 shows a schematic diagram of the laser's optical path. The laser is polarized in tn the plane of the optical table. The first optic encountered by the laser is a 95%-5% beam splitter. The stronger 95% beam (which we refer to as the ionizing beam) is then directed around the experiment and focused into our gas jet.

The weaker 5% beam is first directed into a slightly misaligned Michelson-Morley Interferometer. The mirror pair that directs the beam into the interferometer is on a moveable 1 m delay stage. There are two beams coming out of the interferometer which are slightly out of phase with each other. They are referred to as the probe and reference beams. These beams pass through a half-wave plate that gives them polarization perpendicular to the surface of the table. The beams are then recombined with the ionizing beam on a 50%-50% beam splitter, whereupon they proceed towards the gas jet with the ionizing beam.

Depending on the delay stage position, the probe and reference beam arrive at varying times

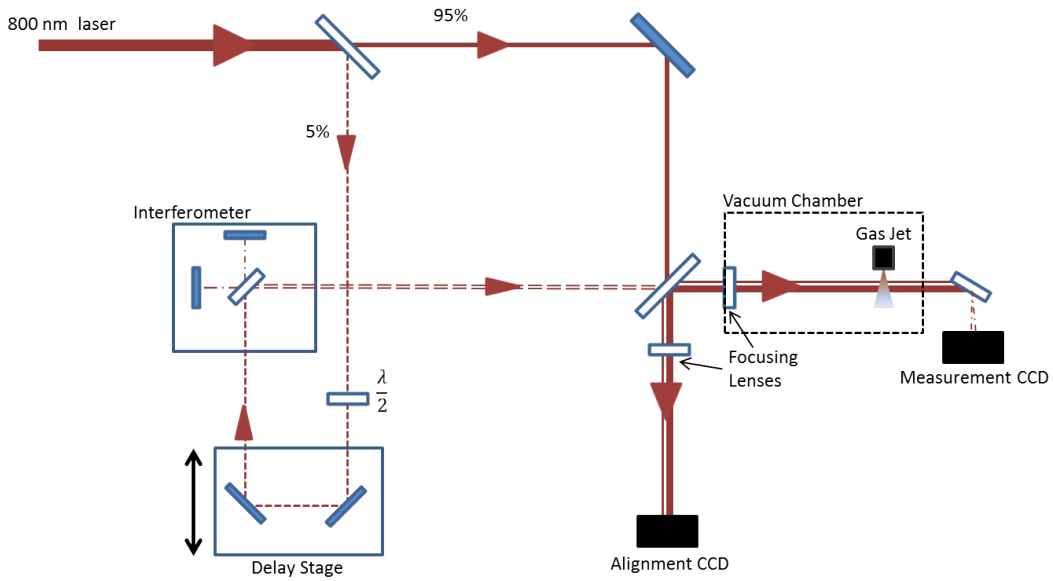

Figure 2.1 The set up of our experiment. The geometry has been simplified to save space and is slightly different than the actual set up.

after the ionization of the plasma has taken place. The probe beam passes through the plasma, and the reference beam passes just outside of the plasma. These two beams overlap in the far field and interfere with one another. The resulting interference pattern is viewed on our measurement CCD camera.

2.2 Alignment Procedures

A large element of our experiment is proper alignment. It is essential that the probe beam passes right through the plasma, and that the reference beam does not. It also is very important that the ionizing beam is centered in the gas jet.

When the ionizing beam is recombined with the probe and reference beams, it is on a 50%-50% beam splitter. So half of the total beam intensity goes to the vacuum chamber, and the other half goes to an alignment camera. The ionizing beam is much stronger than the probe and reference beams. To deal with this power mismatch we use an un-coated optic close to Brewster's angle. All

three laser beams reflect off of this optic. This cuts the intensity of our ionizing beam substantially without having such a strong affect on the other two beams.

The three beams are now at nearly the same intensity. They all pass through a lens and are focused on the alignment camera. We then align the ionizing and probe beams so that they overlap on the camera using only the 50%-50% beam splitter to adjust them. Because of the symmetry of our set up, if the beams are perfectly aligned on the camera, they will also be aligned at the focus of the lens in the gas jet. We overlay the probe and ionizing beam and offset the reference beam.

We also use the polarization of the light to minimize the ionization laser beam intensity on the measurement camera after the vacuum system. The laser beams are directed to the camera by another un-coated optic near Brewster's angle, so that the interference fringes are reflected and the ionizing beam is dramatically reduced. This once again protects our camera and allows us to observe the interference fringes due to the probe and reference beams, while mitigating the background light from the ionizing beam.

2.3 Data Processing

When we were taking data, the information of interest was the phase shift in the interference pattern due to a plasma, relative the interference pattern when there was no plasma. This was detectable as a pixel shift in the fringe pattern on our measurement CCD camera. Figure 2.2has at the top an image of fringes with a plasma, and at the bottom an image with no plasma present. We would align our system and then run a LabVIEW program to store the image of our fringes. The LabVIEW program would record images when there was a plasma and when there was no plasma a designated number of times and would store the information.

Originally the LabVIEW program would tell the user to either "block" or "un-block" the ionizing beam, and then the user would manually tell the computer when this was done. This was a very

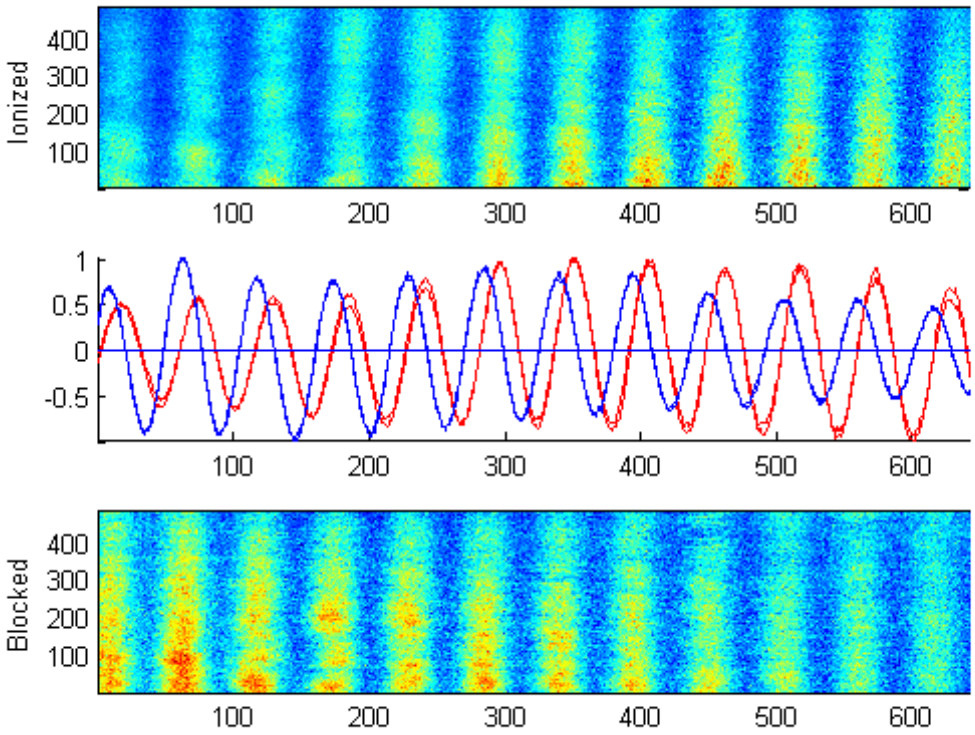

Figure 2.2 An example from a data set where you can see the ionized and unionized data sets with their corresponding sinusoids. The sinusoids are analyzed to find the phase shift $\Delta\phi$. The x axes on the fringes are pixel number, and on the sinusoids the x-axis is pixel number and the y-axis is normalized intensity.

time consuming method with a large margin for user error in the taking of data. It also extended the amount of time associated with a single data set, allowing for possible fluctuations in our setup. To fix this problem we made beam blocks connected to solenoids that could be controlled by LabVIEW. That way the blocking of the beams was controlled by the computer making the process faster and more reliable.

Once the computer had stored the images and we were done taking data we processed the data using a Matlab script. The digital images were viewed as an array of numbers and columns of numbers were averaged to create a sinusoidal representation of the fringe intensity. We did this

with the two sets of fringes (with and without plasma) and then found the average pixel shift from the ionized and un-ionized data. We also calculated the average width of the fringes and divided the shift into that width to find the phase difference $\Delta\phi$ between the two data sets, with one sinusoidal period equal to a phase shift of 2π. Figure 2.2 shows an image of fringes and their corresponding Matlab graphs.

Knowing $\Delta\phi$ allows us to extract the density $n(t)$ of our plasma using the relationship

$$\Delta\phi(t) = \frac{2\pi L}{\lambda}[1-\tilde{n}(t)] \approx n(t)L\frac{q_e^2}{2m_i\varepsilon_0\omega c}$$

in which $\tilde{n}(t)$ is the time evolving index of refraction of the plasma, L is the length of the plasma, m_i is the mass of the ions, and ω is the frequency of our laser, and λ is its wavelength [4]. The time evolving plasma density can be used to extract the electron temperature via the expansion velocity of the plasma. The actual relationship between the density $n(t)$ and the expansion velocity v_{exp} will be discussed in Chapter 3.

Finding the pixel shift between the graphs turned out to be non-trivial, and the method we employed to make it happen is worth mentioning here. First we shifted and normalized the sinusoids in such a way that they were centered about zero in the vertical direction as shown in Figure **??**. This allowed us to determine where the functions would equal zero and then find the pixel shift as a difference in these "zero-crossings".

The way we found the actual zero-crossings was by sending the data into a for loop that took each number in the data set and multiplied it by the next number in the set. If the product was positive it moved on and if the product was negative it saved those two points as a location of a possible zero crossing.

The original Matlab program made in the first iteration of this experiment stopped at this point, but it didn't properly account for possible double crossings as a result of noisy data. To fix this we changed the script so that it identified all the possible zero-crossings and then checked to see if they

were within a few pixels of each other. If they were, it took only the largest of the set of potential crossings. Then it fit a curve to that point, and a few of its neighboors and put the zero-crossing where the curve crossed the horizontal axis. This technique served to make our analysis process more robust than it had previously been, and prevented mistakes in the calculation of ϕ.

With all of this in place we were able to take data. To try and reduce the intensity from test to test, we used an iris diaphragm to clip the edges of our beam. We would take a measurement with different iris diameters at each track length, and then compare the results.

2.4 Preliminary Results

Our initial results were not promising. We found a lot of fluctuation as we ran our experiment from day to day, having difficulties getting our alignment exactly correct each day. The intensity of the laser would drift throughout the day, and as we moved the translation stage from location to location we had difficulty in making the alignment identically consistent.

We also found that since our beam wasn't perfectly Gaussian, when we trimmed the edges with an iris we weren't always reducing the intensity in a consistent way, and our laser focus would move in the vacuum chamber.

Despite these setbacks we were able to reproduce the trends found previously [4] using neon gas with moderate success. We then moved on to using Helium gas thinking that the lighter atoms would expand more quickly in the plasma allowing us to see more of the plasma expansion with the same track length.

However, we didn't see any significant difference between the expansion rates at different ionization intensities. We attributed this to experimental error and took many data sets, but always saw the same thing. A sample of our data can be seen in Figure 2.3.

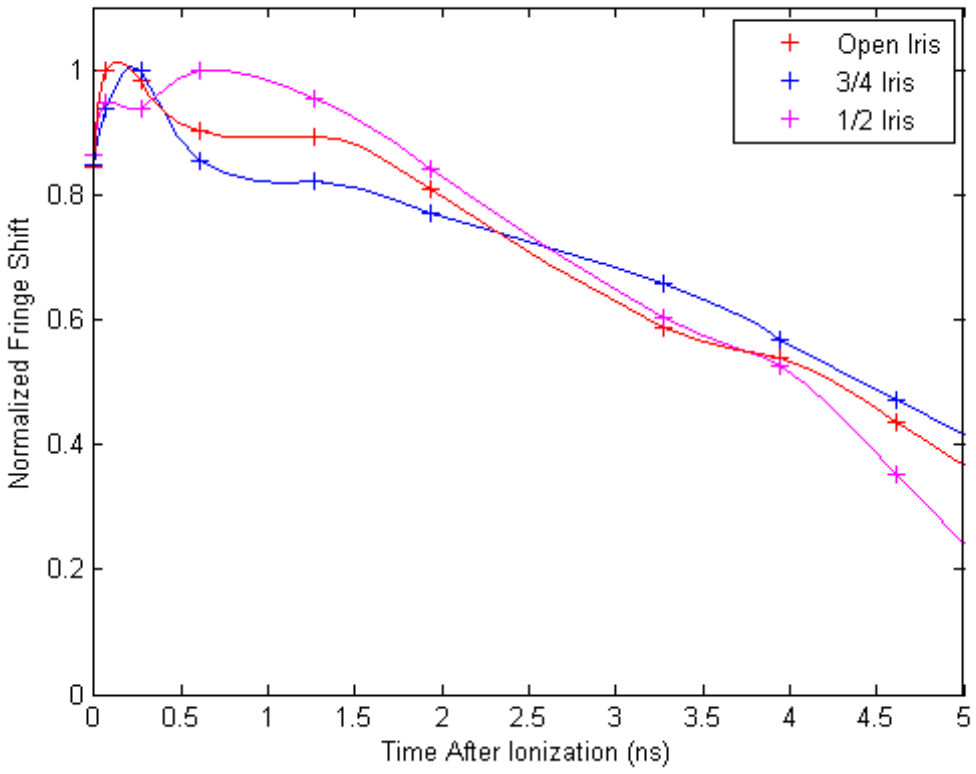

Figure 2.3 Graphs of fringe shifts for 3 different ionization intensities. We are using Helium gas with a backing pressure of 950 torr. Our peak laser intensity is 2.5 $\times 10^{15}$ $W \cdot cm^{-2}$. They are normalized to have the same maximum shift. They are very similar in their trend, and any actual difference is beyond our power to resolve. The crosses are actual data and the lines are just interpolated to emphasize the trend.

Chapter 3

Modeling

3.1 Theory

Before giving up on our attempt at controlling the electron temperature in our LPP we decided to give it a more thorough theoretical look, and to do some modeling to see what exact results we should expect. The results of the modeling we did are very promising for the experiment.

We had expected to see a slower expansion of our plasma as we decreased the ionization energy, but we also expected that plasmas made with a lower intensity would have a lower density, and thus expand more rapidly. The question was, which of these effects would dominate the observed expansion of the plasma.

The intensity of our laser beam was calculated to be 2.5 $\times 10^{15}\ W \cdot cm^{-2}$. The Gaussian width of the focus our ionizing beam is 70 μm [4]. Using this information along with the equations:

$$I_0 = \frac{c\varepsilon_0}{2}|E_0|$$

from [8], and

$$U_p = \frac{q_e^2 E_0^2}{4\omega^2 m_e}$$

$$\langle K_{drift} \rangle = 0.17 U_p = \frac{3}{2} k_b T_e = \frac{3}{2} m_i v_{exp}^2$$

from [4] we are able to extract the expansion velocity v_{exp} of our plasma. In these equations U_p is the Pondermotive energy, T_e is the electron temperature, m_i and m_e are the respective masses of the ion and the electron, I_0 is the intensity at the focus of the ionizing beam, and ω is the laser frequency. All quantities are in SI units.

Once we know v_{exp} we are able to use this equation

$$n(t) = \frac{n(0)}{1 + (v_{exp} t / \sigma_0)^2}$$

to find the density of the plasma as a function of time [6]. In this equation σ_0 is the initial rms size of the plasma.

To find σ_0 we need to figure out how much of our laser focus is intense enough to ionize the gas that we are testing. The first step is figuring out the ionization threshold for strong field ionization. This can be accomplished from a manipulation of equations found in [3]. The intensity is found to be

$$I_{thresh} = \frac{\pi \varepsilon_0^3 c \Phi^4}{2 q_e^6 Z^2}$$

Where Φ is the ionization potential of the atom, and Z is the charge state that will be left behind after ionization [9].

Once we know this intensity threshold we now need to know the intensity profile of our laser beam, so we know how much of it is able to make a plasma. The intensity at the focus of a Gaussian beam is given by

$$I(r) = I_0 e^{-2r^2/w^2}$$

Where r is the radius from the center of the focus and w is the Gaussian beam width [8]. So, σ_0 for our plasma is close to the maximum r_{max} for which $I(r_{max}) = I_{thresh}$.

3.2 Execution

Substituting values back into our equation for the density of the plasma, and dividing by $n(0)$ we get a messy looking equation for the normalized density

$$\frac{n(t)}{n(0)} = \frac{1}{1+Ct^2} \quad \text{where} \quad C = \frac{0.0567 I_0 q_e^2}{\omega^2 m_e m_i c \varepsilon_0 r_{max}^2}.$$

By substituting in the correct values for our laser, and for the gas in question we can plot the normalized density which will have a shape similar to what we would expect for a measurement of our fringe shifts.

The I_{thresh} for Neon and Helium are calculated to be 8.7 $\times 10^{15}$ $W \cdot cm^{-2}$ and 1.3 $\times 10^{15}$ $W \cdot cm^{-2}$ respectively. These intensities, the values of our laser, along with the known values for Φ and m_i, can now be plugged into this equation.

Our modeling was executed in Matlab. We wrote a script that allowed us to choose if we were modeling for Neon or Helium, and let us set a peak intensity I_0 for our laser. It then calculated an r_{max} for the specified values. It plotted the results with different fractions of our peak intensity to see how the plasma densities changed for the different laser beam intensities. We hoped to see the lower intensities fall of more slowly, denoting a slower expansion velocity.

The results for Neon can be seen in Fig. 3.1. We see the decay curves to be very tightly grouped except for 50% which fell of markedly *more quickly*, and 25% which doesn't even show up because it couldn't make any plasma. If you look very closely there is one curve that is decaying more slowly than 100%, but it is close enough that we would never be able to resolve the difference in experiment. Our Helium results, as seen in Fig. 3.2, were even worse. All of the curves decay more quickly for lower intensities, and both 50% and 25% don't make any plasma.

The fact that the plasma expands more quickly for lower intensity is because we are close enough to the threshold intensity that decreasing the intensity in our experiment also decreases plasma size. The smaller plasma is able to expand more quickly, and cancels out the slower expan-

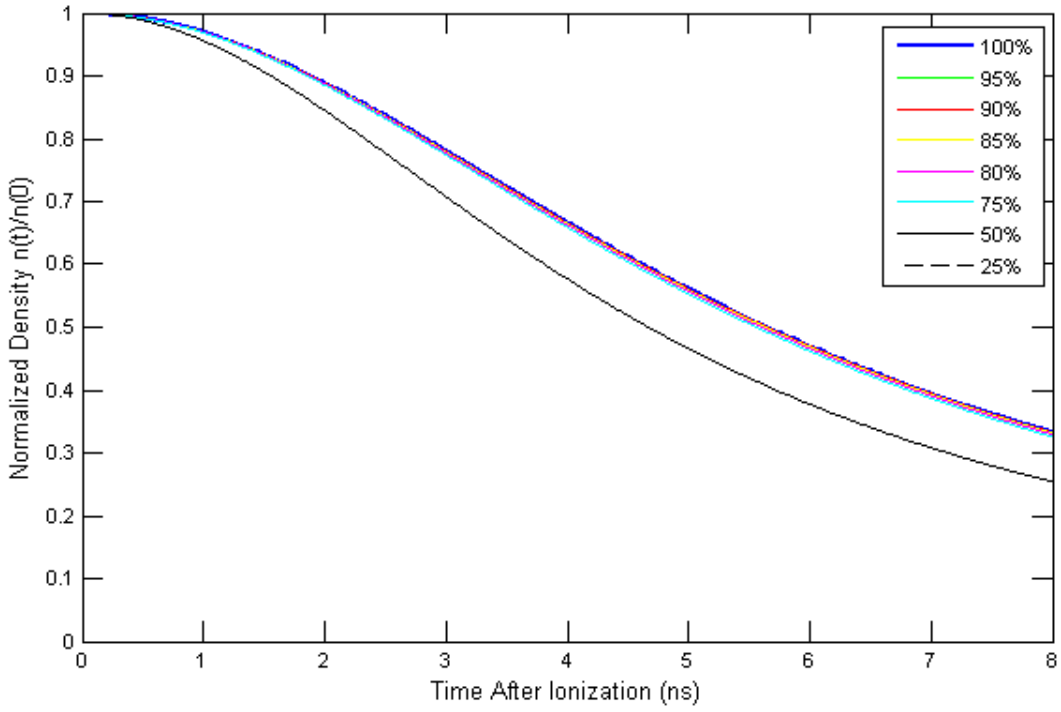

Figure 3.1 A model of our normalized density for neon assuming that I_0 =2.5 $\times 10^{15}$ $W \cdot cm^{-2}$ is the measured value for our laser. The curves are tightly grouped, and as the intensity falls off, the curves decay more quickly contrary to our expectation. The curve for 25% doesn't even make any plasma, and isn't visible on the graph.

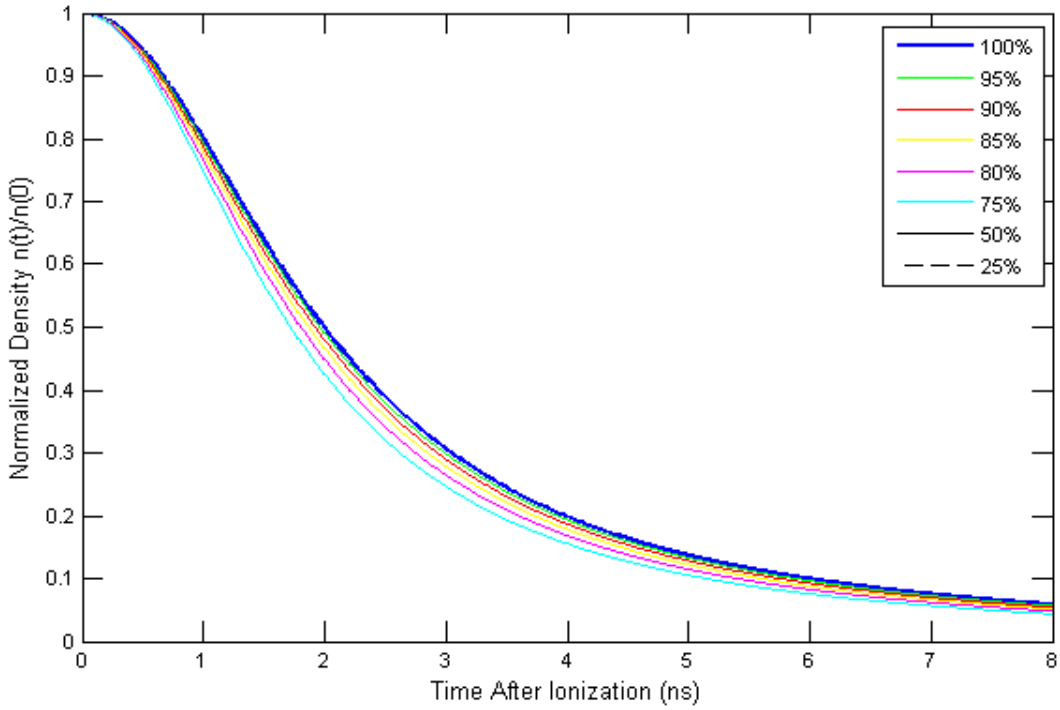

Figure 3.2 A model of our normalized density for helium assuming that $I_0 = 2.5 \times 10^{15}$ $W \cdot cm^{-2}$. The curves aren't as tightly grouped as they are for neon, and the lower intensities decay even more quickly than they did in neon. The plots for 50% and 25% intensities both make no plasma, and so are not visible on the graph.

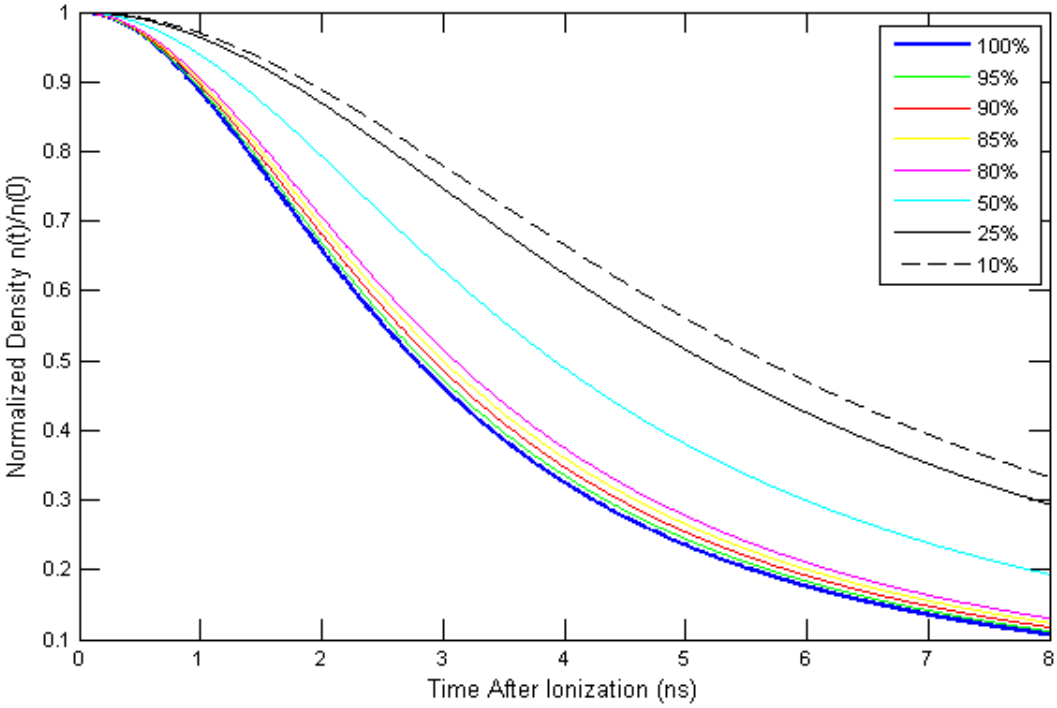

Figure 3.3 A model of our normalized density for neon assuming that I_0 is 10 times higher than what we currently expect, $I_0 = 2.5 \times 10^{16}\ W \cdot cm^{-2}$. The lower intensities expand much more slowly, and the spread would be possible to measure experimentally.

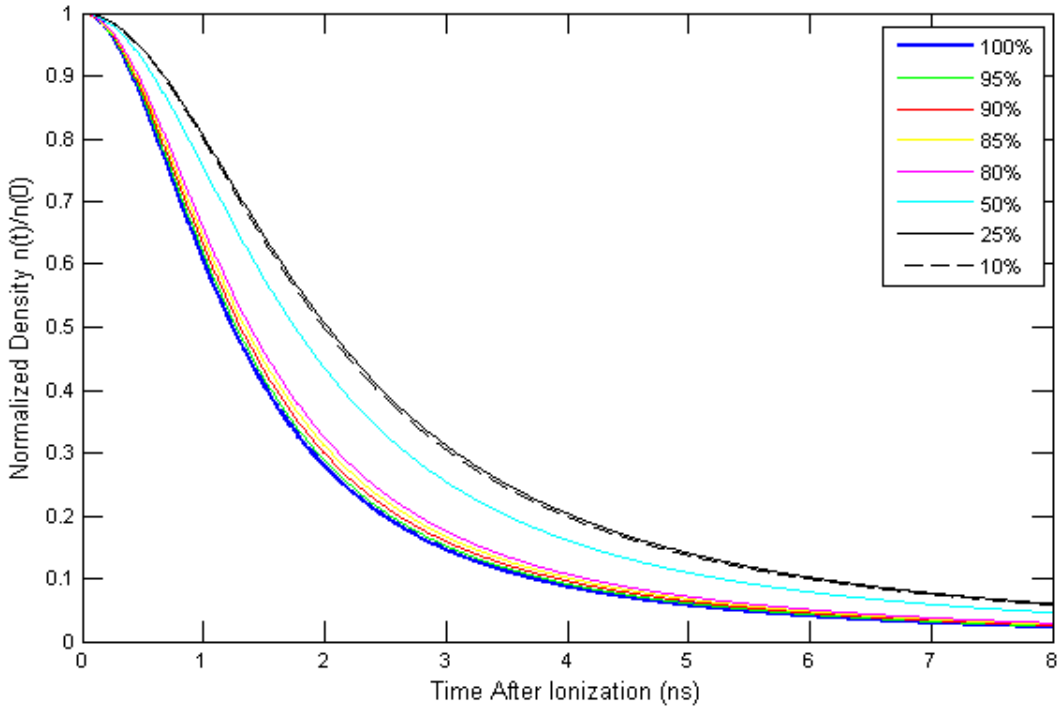

Figure 3.4 A model of our normalized density for helium assuming that I_0 is 10 times higher than what we currently expect, $I_0 = 2.5 \times 10^{16}\ W \cdot cm^{-2}$. The lower intensities expand much more slowly before we get down to 10%, but they spread is tighter. It would be more difficult to measure this difference experimentally.

sion we expected from decreasing intensity.

This suggested that if we increase our laser intensity to get further from the threshold, our plasma size would be more constant, and so we would only see affects from the intensity. It would not be too difficult to increase our ionization intensity by an order of magnitude, so we decided to try again at $I_0 = 2.5 \times 10^{16}\ W \cdot cm^{-2}$. The results in Figures 3.3 and 3.4 were more like what we had hoped for. The neon spreads out beautifully, and the lower intensities have slower expansion. We could very likely measure the the slower expansion experimentally because it seems to be so spread out. The helium also spread out and slowed down, but it is not quite as spaced and would probably be difficult to resolve in our current set up.

Chapter 4

Conclusions and Outlook

After our experiences in the lab and in the modeling it would seem that it is still possible to measure the effect we were hoping to see. Using neon is probably favorable, because at lower intensities of ionization it seems to have greater spacing from the higher intensities than helium does.

Of course for either to work we will need to increase or peak intensity by a factor of 10. This can be accomplished by using a shorter focal length lens. It could also be accomplished by simply increasing the amount of energy in our laser, but this can be difficult to do without damaging optics.

There were other difficulties in the experimental set up that will probably be changed in the next run of the experiment. Our method for curtailing the laser intensity using an iris was inconsistent, and detrimental to alignment. A better approach is to use a half-wave plate followed by a linear polarizer in the beam path as an attenuator. By adjusting the angle of the wave plate relative to the polarizer the intensity of the beam will fall off as $cos^2(2\theta)$ [8] where θ is the angle of the wave plate. This would give us more exact control of the intensity of our laser, and would keep us from moving the focus by diffracting the beam through an iris.

Another difficulty we have had in the experiment is getting the focus of the ionizing beam and probe beam exactly aligned. Upon more informed reflection we realize that we may have had an astigmatism in our focus on our alignment camera. Finding the source and fixing this aberration in

our focus would probably make alignment more simple.

The last thing we would like to try differently as we continue this experiment is the order in which we take data. Instead of trying to take measurements at every track-length in one go, we have contemplated taking a bunch of data sets at each length and then finding an average fringe shift at each length. This would help us overcome the problem of the laser intensity changing throughout a data-taking session and ruining the data.

If these changes are made, the modeling and our experience suggest that this experiment can be successful. We can control the electron temperature and plasma expansion rate in our LPPs by varying the intensity of our laser. Once we have shown this we will be able to move on to other experiments like others currently done only in UNPs, and try to push our plasma to a higher value of Γ.

Bibliography

[1] *Encyclopædia Britannica Encyclopædia Britannica Online Academic Edition* (Encyclopædia Britannica Inc, http://www.britannica.com/EBchecked/topic/457697/photo-ionization, 2013), pp. "photo–ionization".

[2] T. C. Killian, S. Kulin, S. D. Bergeson, L. A. Orozco, C. Orzel, and S. L. Rolston, "Creation of an Ultracold Neutral Plasma," Phys. Rev. Lett. **83,** 4776–4779 (1999).

[3] S. Augst, D. Strickland, D. D. Meyerhofer, S. L. Chin, and J. H. Eberly, "Tunneling ionization of noble gases in a high-intensity laser field," Phys. Rev. Lett. **63,** 2212–2215 (1989).

[4] N. Heilmann, J. B. Peatross, and S. D. Bergeson, ""Ultracold" Neutral Plasmas at Room Temperature," Phys. Rev. Lett. **109,** 035002 (2012).

[5] M. S. Murillo, "Ultrafast dynamics of neutral, ultracold plasmas," PHYSICS OF PLASMAS 14 (2007), 48th Annual Meeting of the Division of Plasma Physics of the APS, Philadelphia, PA, JAN 30-NOV 03, 2006.

[6] S. Laha, P. Gupta, C. E. Simien, H. Gao, J. Castro, T. Pohl, and T. C. Killian, "Experimental Realization of an Exact Solution to the Vlasov Equations for an Expanding Plasma," Phys. Rev. Lett. **99,** 155001 (2007).

[7] T. Kluge, T. Cowan, A. Debus, U. Schramm, K. Zeil, and M. Bussmann, "Electron Temperature Scaling in Laser Interaction with Solids," Phys. Rev. Lett. **107,** 205003 (2011).

[8] J. Peatross and M. Ware, *Physics of Light and Optics*, 2011c ed. (available at optics.byu.edu, 2011).

[9] J. Peatross, Lecture Notes (2013).